MJFAS
Malaysian Journal of Fundamental and Applied Sciences

RESEARCH ARTICLE

Hydrothermally Synthesized Carbon Quantum Dots from *Amomum compactum* for Fluorescence-Based Fe^{3+} Sensing

Said Ali Akbar[a,*], Cut Nuzlia[a], Muhammad Hasan[b]

[a]Department of Aquaculture, Faculty of Marine and Fisheries, Universitas Syiah Kuala, Banda Aceh, 23111, Indonesia.[b]Department of Chemistry Education, Faculty of Teacher Training and Education, Universitas Syiah Kuala, Banda Aceh, 23111, Indonesia

Abstract This study reports the green synthesis of carbon quantum dots (CQDs) derived from *Amomum compactum* via a simple hydrothermal method for the sensitive and selective fluorescence-based detection of Fe^{3+} ions. Compared with previously reported biomass-derived CQD sensors, the developed system offers a simple synthesis route without additional surface modification, high selectivity toward Fe^{3+}, and reliable sensing performance in real water samples. The obtained CQDs exhibit nanoscale dimensions (2.92 nm), strong blue emission, and excitation-dependent optical behavior attributed to quantum confinement effects and abundant oxygen-containing functional groups. These surface characteristics facilitate strong interactions with metal ions, where Fe^{3+} induces a pronounced fluorescence quenching response through coordination interactions and electron transfer with oxygen-containing surface groups, compared to other tested ions, demonstrating high selectivity. The sensing system shows a linear response over a concentration range of 0.001–5 ppm with a low detection limit of 0.085 ppm, which is competitive with several previously reported CQD-based Fe^{3+} fluorescent sensors, meeting requirements for environmental monitoring. Application in real water samples confirms high accuracy and precision, with recovery values ranging from 95.1% to 101.2%. Overall, this work highlights an eco-friendly, cost-effective sensing platform that supports sustainable water quality monitoring, contributing to Sustainable Development Goals (SDGs), particularly SDG 6.

Keywords: carbon quantum dots; *Amomum compactum*; fluorescence sensing; Fe^{3+} detection; environmental monitoring

Introduction

The growing need for detecting trace contaminants in environmental systems has encouraged the exploration of nanoscale fluorescent materials, where carbon quantum dots (CQDs) have gained attention due to their small size and adaptable optical behavior [1,2]. Typically below 10 nm, these carbon-based nanoparticles exhibit strong fluorescence emission, good resistance to photobleaching, and compatibility with aqueous and biological environments. The behavior of CQDs is largely governed by their surface chemistry, where functional groups such as amine, carboxyl, and hydroxyl contribute to enhanced solubility and facilitate interactions with surrounding molecules [3,4]. Unlike conventional materials, the optical response of CQDs is largely governed by quantum confinement and surface defect states, allowing sensitive detection of metal ions even at low concentrations [5]. In addition to their performance, CQDs are also advantageous in terms of synthesis, as they can be produced through various methods including hydrothermal, solvothermal, microwave-assisted, and pyrolytic processes [6]. The use of carbon-rich natural precursors, particularly biomass-derived materials, has become increasingly preferred due to its sustainability and ability to introduce heteroatoms that influence fluorescence behavior [7]. Furthermore, emission properties can be adjusted by modifying synthesis conditions or surface chemistry, providing flexibility in designing CQDs for specific sensing applications across environmental and biological systems.

***For correspondence:**
saidaliakbar@usk.ac.id

Received: 11 April 2026
Accepted: 03 June 2026

Eco-friendly synthesis of carbon quantum dots (CQDs) is increasingly explored to produce materials with high fluorescence efficiency while reducing environmental risks. Natural substances such as carbohydrates, proteins, lipids, and plant-derived metabolites are widely used as sustainable carbon sources [1,8,9]. These raw materials typically yield CQDs with surface groups like hydroxyl and carboxyl that improve solubility in water and contribute to their optical performance [10]. Biomass rich in nitrogen, sulfur, or phosphorus is especially beneficial since heteroatom incorporation can alter the electronic structure and enhance emission properties. Biomass-derived materials are increasingly used as sustainable precursors for CQD synthesis, offering a safer and more economical alternative to conventional methods that rely on harsh chemicals [11,12]. Various agricultural residues have been successfully utilized, however, controlling particle uniformity and maintaining stable optical properties remain challenging. Efforts are therefore focused on improving green synthesis approaches to enhance performance and broaden practical applications [13].

Heavy metals are widely recognized as hazardous pollutants that endanger ecosystems and human well-being, with iron (Fe^{3+}) being of particular concern due to its dual role as both an essential nutrient and a potential toxin [14,15]. Although trace levels of Fe^{3+} are required for normal metabolic functions, excessive concentrations in water can severely disrupt aquatic environments and threaten public health [16]. In fish and other aquatic organisms, high iron exposure alters physiological balance, reduces reproductive performance, and can result in mortality, thereby affecting food chains and ecological stability. For humans, the intake of Fe^{3+}-contaminated water or fish can trigger serious disorders such as liver and kidney damage, oxidative stress, and in extreme cases, fatal outcomes. These risks highlight the urgent need for sensitive and reliable detection of Fe^{3+} in environmental samples, especially drinking water and aquatic systems [17,18]. Fluorescence-based sensing has emerged as a powerful technique for this purpose, offering advantages such as high selectivity, rapid response, and the possibility for real-time analysis. Consequently, the development of fluorescence probes, including those derived from biomass-based carbon quantum dots, represents a promising approach for monitoring and managing iron contamination in the environment [19,20].

Amomum compactum (cardamom) was utilized in this study as a sustainable and economically viable carbon source for the synthesis of carbon quantum dots (CQDs) due to its widespread availability and accessibility, particularly in Indonesia as one of the major producing countries. As a commonly used spice found in both traditional and commercial markets, it provides a continuous and low-cost raw material supply for CQD production. Chemically, *Amomum compactum* is rich in bioactive constituents such as phenolics, flavonoids, terpenoids, and essential oils, which contribute heteroatoms including oxygen and nitrogen that play a key role in the formation of surface functional groups during the synthesis process. These functional groups significantly influence the optical properties, dispersibility, and stability of the resulting CQDs. Furthermore, the presence of aromatic structures containing hydroxyl and methoxy groups enhances fluorescence behavior by facilitating efficient electron transitions and generating diverse emissive surface states. In this work, CQDs were successfully prepared from *Amomum compactum* via a simple hydrothermal method without requiring additional surface modification, resulting in nanoscale particles with abundant surface functionalities favorable for fluorescence emission. Compared with many previously reported biomass-derived CQD systems, the present approach offers a relatively simple and environmentally friendly synthesis route while maintaining competitive sensing performance toward Fe^{3+} ions. In addition, the developed CQDs demonstrated effective fluorescence sensing performance in real water samples without requiring complicated surface engineering or additional chemical passivation steps.The obtained CQDs exhibited excitation-dependent optical behavior, indicating tunable emission properties, and demonstrated strong potential as fluorescence-based sensors, particularly for the detection of Fe^{3+} ions, highlighting their applicability in environmental monitoring.

Materials and Methods

Amomum compactum (cardamom) was used as the carbon precursor. Ultrapure water (resistivity ~18.2 MΩ·cm at 25 °C), produced using a Millipore Simplicity purification system, was used as the solvent in all experiments. Quinine TraceCERT® was obtained from Sigma-Aldrich. Analytical-grade reagents were supplied by Merck, including $ZnCl_2$, $FeCl_3·6H_2O$, $CuSO_4·5H_2O$, $HgCl_2$, $NiCl_2·6H_2O$, $Cr(NO_3)_3·6H_2O$, $PbCl_2$, $SnCl_2·2H_2O$, $CoCl_2·6H_2O$, $AgNO_3$, $CdCl_2·H_2O$, H_2SO_4, $FeCl_2·4H_2O$, HCl, and $Bi_5O(OH)_9(NO_3)_4$, and were used without further purification.

Synthesis of CQDs

The synthesis process was initiated by preparing a homogeneous aqueous suspension of *Amomum compactum* (cardamom), where 2 g of the dried seed powder, previously obtained through mechanical grinding using a laboratory blender, was dispersed in 50 mL of ultrapure water. The resulting mixture was then transferred into a 100 mL Teflon-lined stainless-steel autoclave for hydrothermal treatment. Carbonization was achieved by heating the sealed system at 200 °C for 2 h in a convection oven, after which the reactor was left to cool gradually to room temperature without external intervention. The selected synthesis conditions, including precursor concentration, reaction temperature, and hydrothermal duration, were determined based on preliminary optimization using the Box–Behnken response surface methodology (RSM) to obtain CQDs with favorable fluorescence properties and particle stability. This procedure yielded a dark brown colloidal solution containing carbon quantum dots (CQDs), which was subsequently collected and subjected to further purification and characterization steps.

Instrumentation

The optical response of the prepared samples was first qualitatively examined under UV illumination (365 nm) using a Topcomm LED 2W TP95, and subsequently quantified through emission measurements using a Horiba Scientific FluoroMax. Optical absorption properties were further investigated via UV–vis spectroscopy with a Jenway Genovo Bio, while surface chemical functionalities were identified using FT-IR analysis with a IRXross. To assess particle size distribution and surface charge characteristics, measurements were carried out using a Otsuka Electronics ELSZneo. Structural features at the nanoscale were examined using TEM techniques on a Talos F200X, complemented by Raman spectroscopy using a Horiba iHR320 to analyze carbon structure.

Fluorescence Sensing of Fe^{3+}

A diluted CQD system was first prepared by mixing 100 µL of CQDs with 900 µL of ultrapure water to serve as the base solution for all measurements. For selectivity evaluation, this system was exposed separately to a range of metal ions, including Cu^{2+}, Ni^{2+}, Co^{2+}, Fe^{2+}, Pb^{2+}, Hg^{2+}, Ag^{+}, Cd^{2+}, Zn^{2+}, Sn^{2+}, Cr^{3+}, Bi^{3+}, and Fe^{3+}, each adjusted to a final concentration of 5 ppm. After ion addition, the mixtures were subjected to brief ultrasonic treatment at 40 kHz for 30 s and then left undisturbed at room temperature for 5 min to ensure interaction equilibrium. Following the equilibration step, fluorescence measurements were conducted at an excitation wavelength of 350 nm to evaluate intensity changes caused by different metal ions. To assess detection performance, Fe^{3+} solutions at varying concentrations (0.001–5 ppm) were applied under the same experimental conditions, and the resulting emission variations were examined to understand the quenching behavior and sensitivity of the system.

Visualisation and analysis

Quantitative data obtained from all experiments were statistically evaluated using SPSS version 26, with results expressed in terms of mean ± standard deviation (SD). Graphical representation and data processing were carried out using Origin Pro 2024 to ensure clear visualization of the experimental trends

Results and Discussion

Structural and optical characterization of *Amomum compactum*-derived carbon quantum dots (CQDs)

The micrographs (Fig. 1a–b) clearly show well-dispersed nanoparticles with nearly spherical morphology and no significant agglomeration. The calculated average particle size from HRTEM measurements was approximately 2.92 nm, confirming their classification within the ultra-small nanomaterial range (<10 nm). This nanoscale dimension is crucial, as it directly contributes to the observed optical properties through the quantum confinement effect. The observed lattice fringes in certain regions indicate the coexistence of graphitic domains within a predominantly amorphous carbon framework [22,23]. Such a hybrid arrangement of crystalline and amorphous phases provides active sites for interaction with analytes and enhances surface reactivity. Complementary analysis using FTIR spectroscopy (Fig. 1c) confirmed the presence of abundant oxygen-containing functional groups, including hydroxyl, carboxyl, and carbonyl moieties, which are vital for both water dispersibility and fluorescence modulation [24]. These functional groups not only stabilize the CQDs in aqueous solutions but also serve as coordination sites for metal ions, making the materials highly promising for sensing applications [25,26]. The abundance of oxygen-containing functional groups is believed to play a crucial role in the sensing performance by facilitating strong coordination interactions and electron transfer processes with Fe^{3+} ions, ultimately leading to efficient fluorescence quenching behavior. This structure–property relationship highlights the importance of CQD surface chemistry in governing selectivity and fluorescence response toward target metal ions. The combination of small particle size, uniform distribution, and surface chemistry indicates that *Amomum compactum* CQDs possess favorable characteristics for fluorescence-based detection systems.

Distinct optical behavior of the synthesized CQDs was evidenced by their absorption and emission characteristics. The UV–vis spectrum (Fig. 1d) revealed two prominent absorption features near 255 nm and 324 nm, corresponding to π–π* transitions of aromatic C=C structures and n–π* transitions associated with C=O groups [27,28], indicating the presence of hybrid carbon domains enriched with oxygen-containing functionalities [20]. Under UV excitation, the CQDs produced a strong blue emission centered at 442 nm, and the emission profile exhibited a clear dependence on excitation wavelength, with gradual red-shifts observed as excitation increased, reflecting multiple emissive states and quantum confinement effects (Fig. 1e). Raman analysis further supported the structural features, where the appearance of D (~1336 cm^{-1}) and G (~1590 cm^{-1}) bands confirmed the coexistence of disordered and graphitic carbon structures [15,16,20] (Fig. 1f). The relative intensity of these bands suggests a mixed sp^2/sp^3 hybridization, consistent with nanoscale heterogeneity observed from microscopic analysis. Additional particle size distribution analysis (Fig. 1g) further demonstrated that the synthesized CQDs possessed a relatively narrow nanoscale distribution, confirming the uniformity and stability of the prepared nanomaterials. The combination of these optical and structural characteristics highlights the ability of the CQDs to interact effectively with external species, particularly metal ions, through surface-related processes.

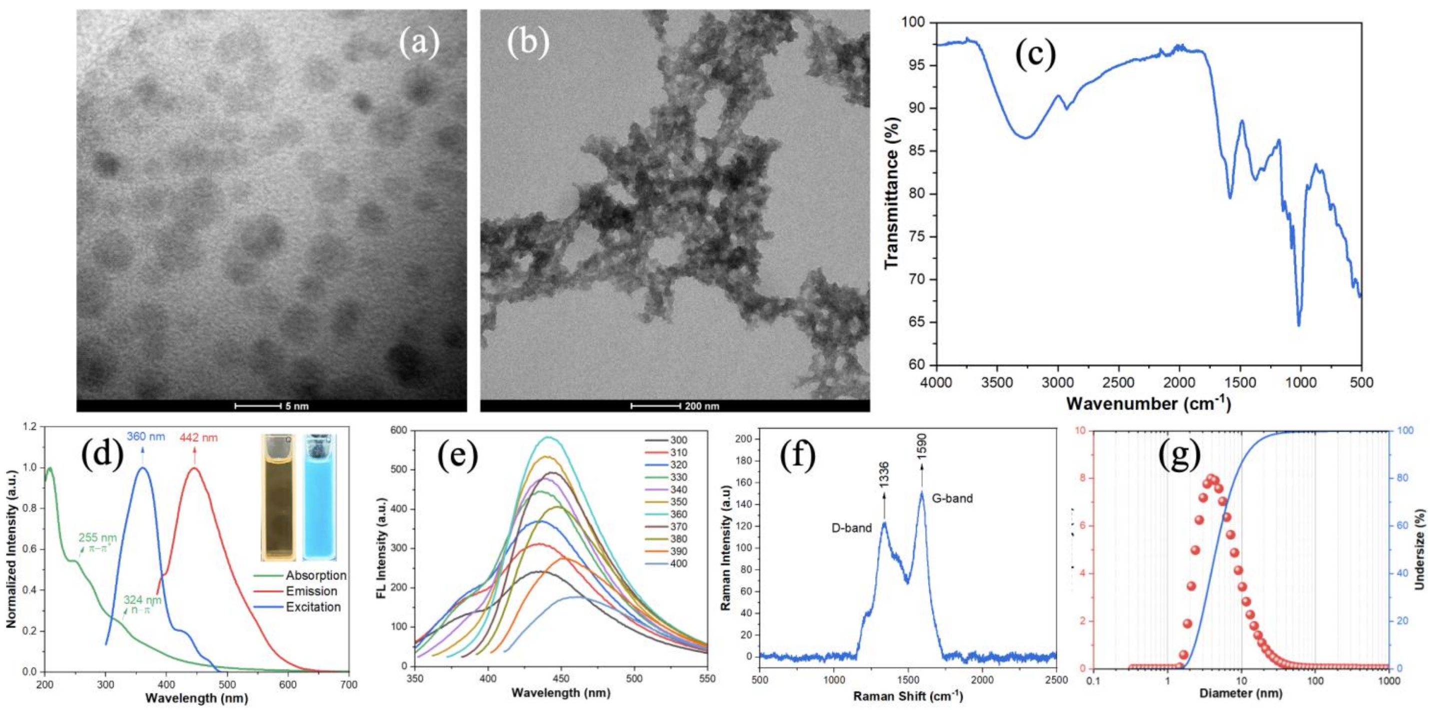

Figure 1. Characterization of carbon dots: (a) HRTEM image at 10 nm scale, (b) HRTEM image at 50 nm scale, (c) FTIR spectrum, (d) UV–Vis absorption and fluorescence spectra, (e) excitation-dependent fluorescence spectra, f) raman spectrum, and (g) particle size distribution

Selectivity and sensitivity of *Amomum compactum*-derived CQDs toward Fe^{3+} ions.

The fluorescence selectivity of *Amomum compactum*-derived carbon quantum dots (CQDs) toward various metal ions was systematically evaluated, as illustrated in Fig. 2a. Among the tested ions, including Ni^{2+}, Cu^{2+}, Fe^{2+}, Co^{2+}, Bi^{3+}, Pb^{2+}, Hg^{2+}, Ag^{+}, Cd^{2+}, Sn^{2+}, Zn^{2+}, and Cr^{3+}, the most significant quenching effect on the CQDs fluorescence was observed in the presence of Fe^{3+}. This strong quenching behavior can be attributed to the high charge density and strong coordination ability of Fe^{3+}, which facilitates electron or energy transfer between Fe^{3+} ions and the surface functional groups of the CQDs, particularly carboxyl and hydroxyl moieties. Such interaction leads to non-radiative recombination of photoexcited electrons and holes, thus reducing fluorescence intensity [4,5]. The negligible effect of other tested ions highlights the remarkable selectivity of CQDs for Fe^{3+} detection, which is a crucial factor for practical sensing applications in complex environmental and biological samples [10,12]. The preferential quenching response toward Fe^{3+} confirms that the oxygen-rich functional groups identified by FTIR are actively involved in ion binding. This selectivity not only underscores the unique surface chemistry of *Amomum compactum*-derived CQDs but also supports their potential as effective fluorescent probes in monitoring iron contamination, especially in drinking water and aquatic systems where interference from other cations is common.

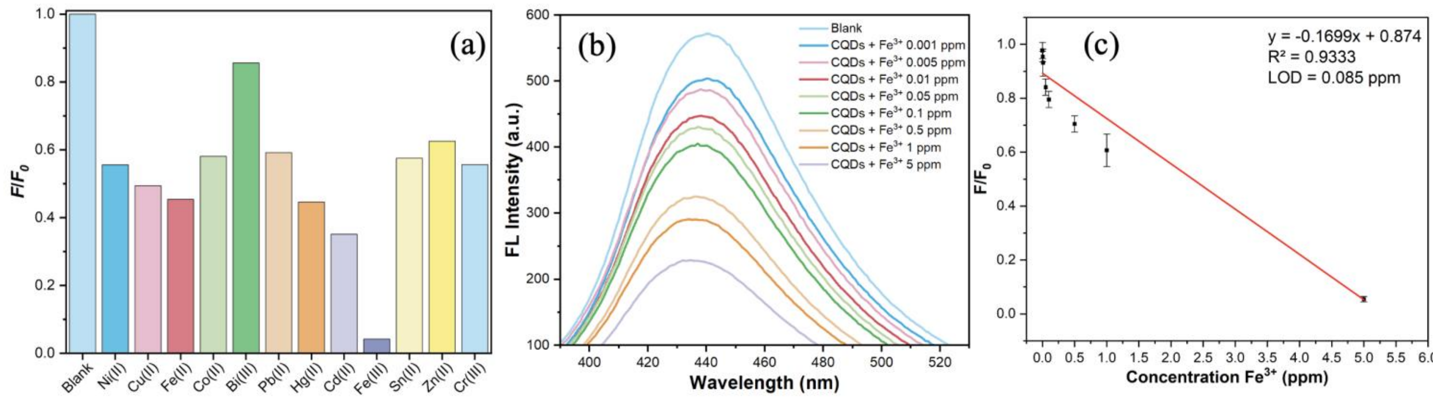

Figure 2. Fluorescence characterization of CQDs: (a) selectivity test of CQDs against various metal ions, (b) fluorescence spectra of CQDs in the presence of Fe^{3+} at different concentrations (0.001–5 ppm), and (c) linear fitting plot of CQDs with Fe^{3+} (0.001–5 ppm)

Fluorescence measurements performed at varying Fe^{3+} concentrations (0.001–5 ppm) revealed a progressive reduction in emission intensity at 442 nm, indicating effective quenching behavior. The relationship between fluorescence response and Fe^{3+} concentration was further analyzed through the Stern–Volmer plot, where a linear correlation between F/F_0 and ion concentration was observed within the tested range, yielding a correlation coefficient (R^2) of 0.933. Although the R^2 value indicates a reasonably good linear relationship, slight deviations from ideal linearity may occur due to heterogeneous surface binding sites, partial aggregation of CQD–Fe^{3+} complexes, and variations in surface-active functional groups at increasing Fe^{3+} concentrations. The detection limit was determined to be 0.085 ppm, which is significantly lower than the recommended maximum concentration for iron in potable water set by international health standards. These results indicate that the CQDs are capable of identifying Fe^{3+} at trace levels suitable for environmental applications. The observed linear response and low detection threshold imply that the quenching process is dominated by strong binding interactions, likely involving coordination between Fe^{3+} ions and surface-active sites of the CQDs, rather than simple collisional mechanisms. Beyond 5 ppm, a deviation from linearity was noted, which may be due to surface saturation of binding sites or aggregation of CQD–Fe^{3+} complexes at higher ion concentrations. These results confirm that *Amomum compactum*-derived CQDs offer both high selectivity and excellent sensitivity for Fe^{3+} detection, positioning them as a promising eco-friendly sensor platform. Compared with several previously reported biomass-derived CQD sensors, the developed system demonstrates competitive analytical performance, particularly in terms of low detection limit, broad detection range, and successful application in real water samples without requiring additional surface functionalization or complex synthesis procedures. The simple hydrothermal synthesis and stable sensing response further highlight the practical advantages of the present CQD system for environmental monitoring applications. Their ability to function effectively at low Fe^{3+} concentrations ensures relevance for real-world applications, such as water quality assessment and monitoring heavy metal contamination in aquatic environments.

Fluorescence lifetime decay and Stern–Volmer analysis of CQDs in the presence of Fe^{3+} ions.

Time-resolved fluorescence spectroscopy was employed to elucidate the quenching mechanism of *Amomum compactum*-derived CQDs in the presence of Fe^{3+} ions. The fluorescence decay profiles (Fig. 3a) revealed a clear reduction in average lifetime after Fe^{3+} addition compared to pristine CQDs. The control sample exhibited a longer decay time, indicating efficient radiative recombination of photogenerated electron–hole pairs. Upon interaction with Fe^{3+} ions, the decay curve shifted significantly, demonstrating faster non-radiative relaxation pathways. This reduction in lifetime suggests that quenching is not solely caused by collisional interactions but also involves electron transfer or complexation between Fe^{3+} and surface functional groups of the CQDs, such as –OH, –COOH, and –C=O. The high charge density of Fe^{3+} facilitates strong binding, which disrupts the emissive states of the CQDs and accelerates non-radiative recombination. The observed trend supports a static or combined static–dynamic quenching mechanism, in line with other reports of metal ion–CQD interactions. This finding emphasizes the crucial role of surface chemistry in dictating quenching behavior and confirms that the functionalized surface of the CQDs is highly responsive to Fe^{3+} coordination.

The relationship between fluorescence intensity and Fe^{3+} concentration was evaluated using the Stern–Volmer model (Fig. 3b), where the F_0/F plot revealed a noticeable deviation from linearity at elevated concentrations. This behavior indicates that the quenching process cannot be attributed to a single mechanism, but rather involves a combination of static and dynamic interactions. The calculated Stern–Volmer constant (Ksv) of 2.5026 suggests a strong affinity between Fe^{3+} ions and the CQD surface. Additionally, the fitting parameter (f_1 = 0.8) together with the correlation coefficient (R^2 = 0.887) demonstrates that the model provides a reasonable representation of the quenching behavior within the studied concentration range. The relatively moderate R^2 value may be attributed to the coexistence of static and dynamic quenching mechanisms, heterogeneous surface-active sites, and partial aggregation of Fe^{3+}–CQD complexes at elevated ion concentrations, which can lead to deviations from ideal linear behavior. At lower Fe^{3+} concentrations (<0.2 ppm), the quenching followed a near-linear response, indicating that initial quenching is dominated by efficient complex formation at active binding sites. However, at higher concentrations (>0.5 ppm), the response deviated from linearity, likely due to surface saturation and aggregation of Fe^{3+}–CQD complexes, which alter the electronic environment and reduce uniform accessibility of active sites [12,13]. These observations further validate that Fe^{3+} ions interact strongly with surface functionalities, leading to fluorescence suppression through electron transfer pathways [17,18]. Collectively, the fluorescence decay and Stern–Volmer analyses provide compelling evidence that *Amomum compactum*-derived CQDs exhibit a highly sensitive and specific response to Fe^{3+} ions, supporting their suitability as effective probes for environmental monitoring.

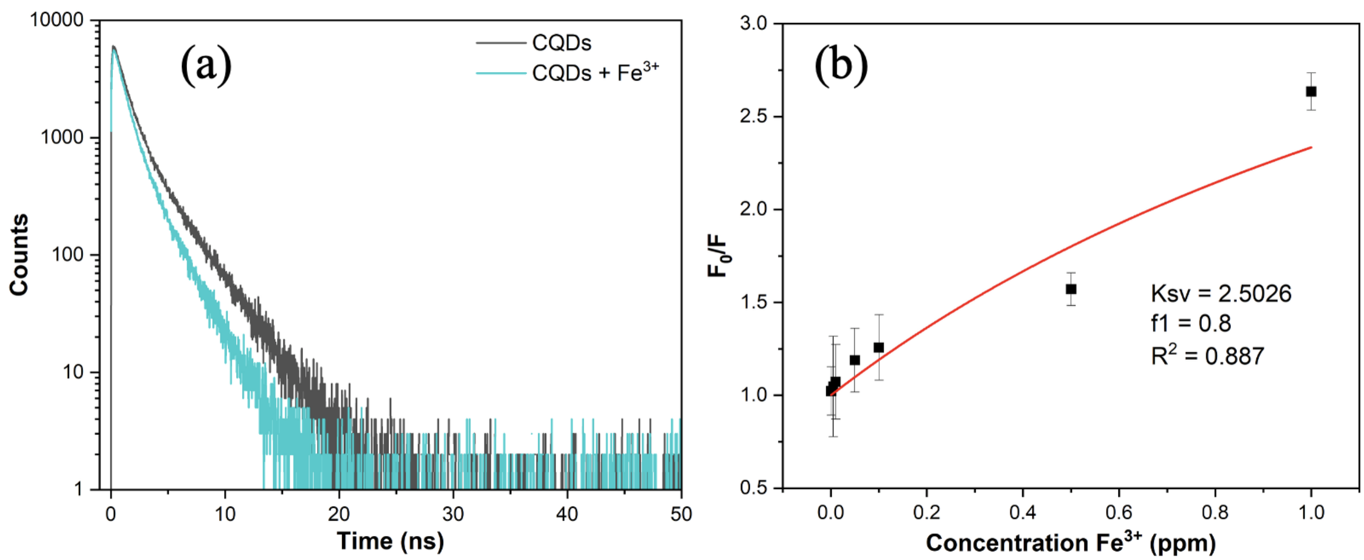

Figure 3. Observation of (a) fluorescence decay curves of CQDs and CQDs with Fe^{3+}, and (b) Stern–Volmer fluorescence quenching profile for Fe^{3+} detection.

Recovery study of Fe^{3+} detection in real water samples

The recovery experiments performed with tap and underground water samples provide a clear indication of the practical applicability of *Amomum compactum*-derived CQDs for real-world sensing of Fe^{3+} ions (Table 1). The recovery values obtained ranged from 95.1% to 101.2% for both types of water, demonstrating excellent analytical accuracy and reliability of the proposed method. At the lowest spiked concentration (0.005 ppm), recoveries were consistently close to 100%, confirming that the CQDs are highly effective in detecting Fe^{3+} even at trace levels well below the World Health Organization (WHO) limit of 0.3 ppm for drinking water. As the spiking concentration increased, recovery values remained stable, with only slight deviations observed at higher levels (0.5–1 ppm), which may be attributed to partial saturation of available surface binding sites or matrix effects from dissolved ions in natural water [14,23]. Importantly, the relative standard deviation (RSD) values across all concentrations were below 1%, indicating excellent reproducibility and precision in the measurements. The consistency of these results across two different water sources suggests that the CQD-based sensor is not significantly affected by common coexisting ions or natural organic matter typically present in environmental waters. This robustness is essential for reliable application in diverse water quality monitoring contexts [22,29,30, 31,32]. The slight differences between tap and underground water recoveries may be due to variations in the ionic composition and mineral content of the matrices; nevertheless, both fell within the acceptable analytical range. Taken together, the high recovery rates, low RSD values, and sensitive detection performance underscore the strong potential of *Amomum compactum*-derived CQDs as a cost-effective, eco-friendly, and highly reliable fluorescence probe for monitoring Fe^{3+} contamination in environmental water systems.

Table 1. Analytical Performance of Fe^{3+} Detection in Real Water Samples

Water samples	Added (ppm)	RSD (%)	Recovery (%)	Measured (ppm)
Underground water	0.005	0.68	99.1	0.0049 ± 0.0001
	0.01	0.74	101.0	0.0101 ± 0.0002
	0.05	0.28	99.6	0.0498 ± 0.0005
	0.1	0.15	98.5	0.0985 ± 0.0007
	0.5	0.21	96.4	0.482 ± 0.004
	1	0.39	95.1	0.951 ± 0.005
Tap water	0.005	0.78	101.2	0.0051 ± 0.0001
	0.01	0.70	98.5	0.0098 ± 0.0002
	0.05	0.22	100.6	0.0503 ± 0.0004
	0.1	0.63	99.0	0.0990 ± 0.0006
	0.5	0.55	98.8	0.494 ± 0.003
	1	0.59	95.6	0.956 ± 0.006

Comparison with previously reported biomass-derived CQD sensors for Fe^{3+} detection

Table 2 presents a comparative overview of recently reported biomass-derived carbon quantum dots (CQDs) used for fluorescence-based Fe^{3+} sensing applications. The comparison highlights differences in carbon precursor, synthesis strategy, particle size, quantum yield, and analytical sensitivity represented by the limit of detection (LOD). Most previously reported CQDs were synthesized through hydrothermal methods using various natural precursors such as *Borassus flabellifer* [35], elm seeds [36], canistel (*Pouteria campechiana*) [37], papaya powder [40], soybean [42], sugarcane molasses [43], and *Magnolia liliiflora* flower [41], demonstrating the increasing interest in sustainable biomass resources for fluorescent nanomaterial production. Other synthesis approaches, including pyrolyzation with oxygenolysis [38], ultrasonic-assisted synthesis [42], microwave heating [44], and carbonization-assisted ultrasonication [14], have also been reported to enhance CQD formation and sensing performance. The average particle sizes generally ranged from approximately 1.9 to 10.8 nm, indicating that nanoscale dimensions are commonly associated with favorable fluorescence behavior and metal ion sensing efficiency. However, significant variation in quantum yield and LOD values was observed among the reported systems, suggesting that precursor composition and synthesis conditions strongly influence optical and analytical properties. The *Amomum Compactum*-derived CQDs developed in the present work exhibited an average particle size of approximately 2.92 nm with a quantum yield of 10.85% and an LOD value of 1.52 µM. Although several previously reported CQDs demonstrated lower LOD values, particularly papaya-derived CQDs (0.48 µM) [40] and *Syzygium Aromaticum*-derived CQDs (0.515 µM) [14], the present CQDs remain highly competitive considering their simple hydrothermal synthesis route, absence of additional surface functionalization, and stable sensing performance in real water samples.

Furthermore, the developed CQDs demonstrated excellent selectivity toward Fe^{3+} ions together with satisfactory recovery values ranging from 95.1% to 101.2%, confirming their practical applicability for environmental monitoring. Overall, the comparative analysis confirms that *Amomum compactum*-derived CQDs represent a promising addition to the growing class of sustainable fluorescent nanomaterials for selective Fe^{3+} sensing applications.

Table 2. Comparison of biomass-derived carbon quantum dots for Fe^{3+} sensing applications

No	Carbon source	Synthesis method	Average size (nm)	Quantum yield (%)	LOD values (μM)	References
1	*Borassus flabellifer*	Hydrothermal	2–7	19.4	2.01	[33]
2	Elm seeds	Hydrothermal	3.83	6.15	3.18	[34]
3	Canistel (*Pouteria campechiana*)	Hydrothermal	~8.1	1.24	19.0	[35]
4	Mango-peel	Pyrolyzation with oxygenolysis	2–6	8.5 ± 0.2	1.2	[36]
5	Cranberry beans	Hydrothermal	1.23–6.63	10.85	9.55	[37]
6	Papaya powder	Hydrothermal	3.4–10.8	18.98	0.48	[38]
7	*Magnolia liliiflora* flower	Hydrothermal	4 ± 1	11	1.2	[39]
8	Soybeans	Ultrasonic	2.4	16.7	2.9	[40]
9	Sugarcane molasses	Hydrothermal	1.9	5.8	1.46	[41]
10	Grilled turbot fish	Microwave heating	3–5	1.67	3.96	[42]
11	*Syzygium aromaticum*	Carbonization-assisted ultrasonication	3.314	12.61	0.515	[14]
12	*Amomum compactum*	Hydrothermal	(~2.92 nm)	10.85	1.52	This work

Conclusions

A fluorescence-based sensing approach was successfully developed using carbon quantum dots derived from *Amomum compactum* (cardamom) as a sustainable and naturally abundant precursor through a simple hydrothermal synthesis route without additional surface modification. The resulting CQDs exhibited stable optical behavior characterized by strong blue emission, excitation-dependent fluorescence properties, nanoscale dimensions (~2.92 nm), and oxygen-rich surface functionalities that promoted selective interaction with Fe^{3+} ions. The developed sensing system demonstrated a sensitive fluorescence quenching response toward Fe^{3+} through coordination interactions and electron transfer processes involving surface functional groups. Quantitative analysis revealed a linear detection range of 0.001–5 ppm with a low detection limit of 0.085 ppm and a correlation coefficient (R^2) of 0.933, indicating good analytical performance for trace-level Fe^{3+} detection in environmental waters. Stern–Volmer analysis further confirmed strong interactions between Fe^{3+} and the CQD surface, with a quenching constant (Ksv) of 2.5026. Application in real water samples showed satisfactory recovery values ranging from 95.1% to 101.2% with low RSD values, confirming good accuracy, reproducibility, and practical applicability. Overall, the developed biomass-derived CQDs provide a cost-effective, eco-friendly, and competitive fluorescent sensing platform for selective Fe^{3+} monitoring in environmental systems.

Conflicts of Interest

The authors declare that there is no conflict of interest regarding the publication of this paper.

Acknowledgment

This work was supported by the Directorate of Research and Community Service, Ministry of Education, Science, and Technology of the Republic of Indonesia, under the Fundamental Research Program (Regular Scheme), Fiscal Year 2025 (Contract No. 113/C3/DT.05.00/PL/2025).

References

[1] Han, Y., Li, M., Zheng, J., Wei, L., & Zhu, L. (2022). Green conversion of excess sludge to N-Ca self-doping sustainable carbon quantum dots with remarkable fluorescence enhancement and residual heavy metal reduction. *Journal of Environmental Chemical Engineering, 10*, 108934. https://doi.org/10.1016/j.jece.2022.108934

[2] You, X.-Y., Yin, W.-M., Wang, Y., Wang, C., Zheng, W.-X., & Guo, Y.-R. (2024). Enrichment and immobilization of heavy metal ions from wastewater by nanocellulose/carbon dots-derived composite. *International Journal of Biological Macromolecules, 255*, 128274. https://doi.org/10.1016/j.ijbiomac.2023.128274

[3] Zhang, J., Wang, Q., Wan, H., Shi, Y., & Huang, L. (2023). Enhanced etching terminal wastewater treatment and H_2 production by in-situ deposited heavy metals on carbon dots/g-C_3N_4 photocathode microbial electrolysis cells. *Journal of Hazardous Materials, 459*, 132178. https://doi.org/10.1016/j.jhazmat.2023.132178

[4] Obayes, H. K., Meteab, M. H., & Al-Kareem, B. A. (2024). Modified dosimetric features of new type of lithium borate glass system: Role of magnesium and gold Co-doping. *Transactions on Electrical and Electronic Materials*, *25*(6), 708-721. https://doi.org/10.1007/s42341-024-00551-2

[5] Sami, N. A., Nattah, A. M., Jawad, R. A., Meteab, M. H., & Mohammed, M. K. (2025). Modification and Enhancement of The Structural, Morphological and Optical Characteristics of PMMA/In2O3/SiO2 Promising Ternary Nanostructures for Optical Nanodevices and Gamma Ray Attenuation. *Trends in Sciences*, *22*(7), 9959-9959. https://doi.org/10.48048/tis.2025.9959

[6] Ananda, B., Krushna, B. R. R., Sharma, S. C., Salwe, K. J., Sharma, R., & Akkara, P. J. (2025). Microwave enhanced carbon dots synthesis from eggshell membrane: Versatile applications in heavy metal ion sensing, strain free detection of fingerprints, UV shielding, food packing and anti-counterfeiting. *Colloids and Surfaces A: Physicochemical and Engineering Aspects, 705*, 135740. https://doi.org/10.1016/j.colsurfa.2024.135740

[7] Bhattacharjee, T., Konwar, A., Boruah, J. S., Chowdhury, D., & Majumdar, G. (2023). A sustainable approach for heavy metal remediation from water using carbon dot based composites: A review. *Journal of Hazardous Materials Advances, 10*, 100295. https://doi.org/10.1016/j.hazadv.2023.100295

[8] Hadi, A. N., Meteab, M. H., & Mohammed, M. K. (2025). Influence of Inclusion Sb2O3/NiO Nanostructures on the Morphological, Microstructural, and Optical Characteristics of PVA Polymeric for Gamma-Ray Shielding Applications. *Revue des Composites et des Materiaux Avances*, *35*(3), 581. https://doi.org/10.18280/rcma.350319

[9] Koparde, S. V., Nille, O. S., Kolekar, A. G., Bote, P. P., Gaikwad, K. V., & Anbhule, P. V. (2024). Okra peel-derived nitrogen-doped carbon dots: Eco-friendly synthesis and multi-functional applications in heavy metal ion sensing, nitro compound detection and environmental remediation. *Spectrochimica Acta Part A: Molecular and Biomolecular Spectroscopy, 321*, 124659. https://doi.org/10.1016/j.saa.2024.124659

[10] Aygun, A., Cobas, I., Tiri, R. N. E., & Sen, F. (2024). Hydrothermal synthesis of B, S, and N-doped carbon quantum dots for colorimetric sensing of heavy metal ions. *RSC Advances, 14*, 10814–10825. https://doi.org/10.1039/d4ra00397g

[11] Algethami, F. K., & Abdelhamid, H. N. (2024). Heteroatoms-doped carbon dots as dual probes for heavy metal detection. *Talanta, 273*, 125893. https://doi.org/10.1016/j.talanta.2024.125893

[12] Baruah, S., Hazarika, P., Konwar, A., Hazarika, K. K., & Hazarika, S. (2025). Corrigendum to “Synergistic optical sensing of heavy metal ions using Mesua ferrea-derived carbon dot embedded alginate based biopolymeric film as a sensor platform”. *International Journal of Biological Macromolecules*. https://doi.org/10.1016/j.ijbiomac.2025.147572

[13] Wang, F., Zhang, Y., Li, H., Gong, W., Han, J., & Jiang, S. (2025). Application of carbon quantum dots as fluorescent probes in the detection of antibiotics and heavy metals. *Food Chemistry, 463*, 141122. https://doi.org/10.1016/j.foodchem.2024.141122

[14] Akbar, S. A., Hasan, M., Nazar, M., Zulfahmi, I., Miswar, E., & Iqhrammullah, M. (2025). Fluorescent carbon quantum dots from *Syzygium aromaticum* as a selective sensor for Fe^{3+} and Cd^{2+} detection in aqueous solution. *Case Studies in Chemical and Environmental Engineering, 11*, 101166. https://doi.org/10.1016/j.cscee.2025.101166

[15] Venkatesan, G., & Sathiyan, G. (2025). Recent trends in use of plant-derived carbon dot-based fluorescent probes for heavy metal ion detection and their biological applications. *Trends in Environmental Analytical Chemistry, 46*, e00259. https://doi.org/10.1016/j.teac.2025.e00259

[16] Yan, F., Liu, S., Huo, X., Liang, G., Yang, F., Zhang, B., & others. (2025). Engineering a carbon dot-decorated fluorescent nanoplatform to promote heavy metal reutilization and photothermal evaporation with antibacterial activity. *Chemical Engineering Journal, 504*, 158890. https://doi.org/10.1016/j.cej.2024.158890

[17] Zhong, W., & Yang, J. (2024). Fluorescent carbon quantum dots for heavy metal sensing. *Science of the Total Environment, 957*, 177473. https://doi.org/10.1016/j.scitotenv.2024.177473

[18] Chobpattana, V., Sangtawesin, T., Khaopueak, P., & Wechakorn, K. (2025). Sugar derived fluorescent carbon quantum dots conjugated glutathione for sensing heavy metal ions and antioxidant activity. *Materials Science and Engineering: B, 313*, 117956. https://doi.org/10.1016/j.mseb.2024.117956

[19] Baruah, S., Hazarika, P., Konwar, A., Hazarika, K. K., & Hazarika, S. (2025). Synergistic optical sensing of heavy metal ions using Mesua ferrea derived carbon dot embedded alginate based biopolymeric film as a sensor platform. *International Journal of Biological Macromolecules, 286*, 138227. https://doi.org/10.1016/j.ijbiomac.2024.138227

[20] Kadhim, K. K., Azeez, H. M., Yousif, R. T., Mohammed, M. K., & Meteab, M. H. (2025). Boosting the structural, optical and AC electrical characteristics of PVA/CdTe nanocomposites for flexible smart optoelectronic devices. *International Journal of Nanoelectronics and Materials (IJNeaM)*, *18*(4), 527-536. https://doi.org/10.58915/ijneam.v18i4.2617

[21] Nurcholis, W., Sya'bani Putri, D. N., Husnawati, H., Aisyah, S. I., & Priosoeryanto, B. P. (2021). Total flavonoid content and antioxidant activity of ethanol and ethyl acetate extracts from accessions of *Amomum compactum* fruits. *Annals of Agricultural Sciences, 66*, 58–62. https://doi.org/10.1016/j.aoas.2021.04.001

[22] Anum, J., Akhtar, M. A., Khan, A. M., Ahmed, K., Sayes, C. M., & Almajwal, A. M. (2025). Green-synthesized amino-rich carbon quantum dots: A dual-function platform for fluorescent detection of heavy metals and degradation of malachite green dye. *Journal of Water Process Engineering, 77*, 108472. https://doi.org/10.1016/j.jwpe.2025.108472

[23] Singh, P., & Singh, L. K. (2025). Carbon quantum dots as a promising tool for heavy metal sensing and removal in wastewater. *Desalination and Water Treatment, 324*, 101435. https://doi.org/10.1016/j.dwt.2025.101435

[24] Srivastava, S. K., Pratap, R., Yadav, M., Mishra, M., Chaudhary, S., & Chawla, R. (2025). Biogenic synthesis of highly stable multifluorescent carbon quantum dots as dual probe sensor for detection of heavy toxic metal ions. *Colloids and Surfaces A: Physicochemical and Engineering Aspects, 723*, 137336. https://doi.org/10.1016/j.colsurfa.2025.137336

[25] Enriquez, B. U. M., Rangel-Ayala, M., Kumar, Y., Garcia, J. E., Gomez-Aguilar, J. F., & Khandual, S. (2025). Multifunctional Arthrospira platensis biomass derived carbon dots: Sensing/removal of heavy metal ions and optoelectronic applications. *Journal of Environmental Chemical Engineering, 13*, 117827. https://doi.org/10.1016/j.jece.2025.117827

[26] Maity, S., Kumar, S., Singh, G., Patra, S., Pareek, D., & Paik, P. (2025). Selective sensing of heavy metal ions using carbon dots synthesized from *Azadirachta indica* seeds. *Sensors and Diagnostics, 4*, 407–415. https://doi.org/10.1039/d4sd00350k

[27] Wu, H., & Gao, H. (2025). Preparation of Auricularia auricula doped carbon-nitrogen quantum dots and their application in detecting heavy metal ions. *Chinese Journal of Analytical Chemistry, 53*, 100596. https://doi.org/10.1016/j.cjac.2025.100596

[28] Javeria, H., Abbas, M. Q., Chen, S.-H., Keshat, B. E., & Du, Z. (2025). Scalability of sulfur-functionalized carbon quantum dots from peanut shells: A sustainable sensor for heavy metal detection. *Journal of Environmental Chemical Engineering, 13*, 115821. https://doi.org/10.1016/j.jece.2025.115821

[29] Akbar, S. A., Zulfahmi, I., Setiawan, I., Jalil, Z., Rahman, M. M., & Lahori, A. H. (2026). Green synthesis of biomass-derived carbon quantum dots from *Syzygium Aromaticum* via carbonization-assisted ultrasonication for a selective colorimetric sensor of Ag^+ in environmental waters. *Applied Science And Engineering Progress, 19*(2), 7925. https://doi.org/10.14416/j.asep.2025.09.011

[30] Akbar, S. A., Irham, M., Hasan, H. A., Zulfahmi, I., Iqbal, T., Ahsan, A., Rahman, M. M., & Jalil, Z. (2026). Fluorescent optical sensor for Fe^{3+} detection using *Syzygium Aromaticum*-derived carbon quantum dots embedded in corn starch biopolymeric film. *International Journal Of Biological Macromolecules*, *359*, 151873. https://doi.org/10.1016/j.ijbiomac.2026.151873

[31] Akbar, S. A., Rochliadi, A., Suendo, V., Saidi, N., Lelifajri, L., & Mardhiah, A. A. (2018). Raman spectroscopy study of the polyaniline electrode on Zn polyaniline rechargeable batteries. *Rasayan J. Chem*, *11*, 1525-1531. http://dx.doi.org/10.31788/RJC.2018.1144064

[32] Akbar, S. A., Hasan, M., Jalil, Z., Zulfahmi, I., Iqhrammullah, M., & Safina, N. (2025). Enhanced ammonia nitrogen filtration using NaOH-activated Manihot utilissima peel carbon: Application in recirculating aquaculture systems for Nile tilapia. *Chemosphere*, *385*, 144537. https://doi.org/10.1016/j.chemosphere.2025.144537

[33] Nagaraj, M., Ramalingam, S., Murugan, C., Aldawood, S., Jin, J. O., Choi, I., & Kim, M. (2022). Detection of Fe^{3+} ions in aqueous environment using fluorescent carbon quantum dots synthesized from endosperm of *Borassus Flabellifer*. *Environmental Research, 212*, 113273. https://doi.org/10.1016/j.envres.2022.113273

[34] Zhang, J., Zheng, G., Tian, Y., Zhang, C., Wang, Y., Liu, M., Ren, D., Sun, H., & Yu, W. (2022). Green synthesis of carbon dots from elm seeds via hydrothermal method for Fe^{3+} detection and cell imaging. *Inorganic Chemistry Communications, 144*, 109837. https://doi.org/10.1016/j.inoche.2022.109837

[35] Quang, N. K., & Son, L. V. T. (2022). Sensitive detection of Fe^{3+} ions and cell imaging of carbon nanodots derived from canistel (*Pouteria Campechiana*). *MRS Advances, 7*, 278–283. https://doi.org/10.1557/s43580-022-00267-6

[36] Jiao, X. Y., Li, L. S., Qin, S., Zhang, Y., Huang, K., & Xu, L. (2019). The synthesis of fluorescent carbon dots from mango peel and their multiple applications. *Colloids And Surfaces A: Physicochemical And Engineering Aspects, 577*, 306–314. https://doi.org/10.1016/j.colsurfa.2019.05.073

[37] Zulfajri, M., Gedda, G., Chang, C. J., Chang, Y. P., & Huang, G. G. (2019). Cranberry beans derived carbon dots as a potential fluorescence sensor for selective detection of Fe^{3+} ions in aqueous solution. *ACS Omega, 4*, 15382–15392. https://doi.org/10.1021/acsomega.9b01333

[38] Wang, N., Wang, Y., Guo, T., Yang, T., Chen, M., & Wang, J. (2016). Green preparation of carbon dots with papaya as carbon source for effective fluorescent sensing of iron (III) and *Escherichia Coli*. *Biosensors And Bioelectronics, 85*, 68–75. https://doi.org/10.1016/j.bios.2016.04.089

[39] Atchudan, R., Edison, T. N. J. I., Aseer, K. R., Perumal, S., & Lee, Y. R. (2018). Hydrothermal conversion of *Magnolia Liliiflora* into nitrogen-doped carbon dots as an effective turn-off fluorescence sensing, multi-colour cell imaging and fluorescent ink. *Colloids And Surfaces B: Biointerfaces, 169*, 321–328. https://doi.org/10.1016/j.colsurfb.2018.05.032

[40] Zhao, W. B., Liu, K. K., Song, S. Y., Zhou, R., & Shan, C. X. (2019). Fluorescent nano-biomass dots: Ultrasonic-assisted extraction and their application as nanoprobe for Fe^{3+} detection. *Nanoscale Research Letters, 14*, 130. https://doi.org/10.1186/s11671-019-2950-x

[41] Huang, G., Chen, X., Wang, C., Zheng, H., Huang, Z., Chen, D., & Xie, H. (2017). Photoluminescent carbon dots derived from sugarcane molasses: Synthesis, properties, and applications. *RSC AdvanceS, 7*, 47840–47847. https://doi.org/10.1039/c7ra09002a

[42] Bi, J., Wang, H., Kamal, T., Zhu, B. W., & Tan, M. (2017). A fluorescence turn-off-on chemosensor based on carbon nanocages for detection of ascorbic acid. *RSC Advances, 7*, 30481–30487. https://doi.org/10.1039/c7ra04394e